

**High-field phase diagram and phase transitions in hexagonal manganite  $\text{ErMnO}_3$** Y. J. Liu,<sup>1</sup> J. F. Wang,<sup>1,\*</sup> X. F. Sun,<sup>2,3,4,†</sup> J.-S. Zhou,<sup>5</sup> Z. C. Xia,<sup>1</sup> Z. W. Ouyang,<sup>1</sup> M. Yang,<sup>1</sup> C. B. Liu,<sup>1</sup> R. Chen,<sup>1</sup> J.-G. Cheng,<sup>6</sup> Y. Kohama,<sup>7</sup> M. Tokunaga,<sup>7</sup> and K. Kindo<sup>7</sup><sup>1</sup>Wuhan National High Magnetic Field Center and School of Physics, Huazhong University of Science and Technology, Wuhan 430074, China<sup>2</sup>Department of Physics, Hefei National Laboratory for Physical Sciences at Microscale, and Key Laboratory of Strongly-Coupled Quantum Matter Physics (CAS), University of Science and Technology of China, Hefei, Anhui 230026, China<sup>3</sup>Institute of Physical Science and Information Technology, Anhui University, Hefei, Anhui 230601, China<sup>4</sup>Collaborative Innovation Center of Advanced Microstructures, Nanjing University, Nanjing, Jiangsu 210093, China<sup>5</sup>Materials Science and Engineering Program, University of Texas at Austin, Austin, Texas 78712, USA<sup>6</sup>Beijing National Laboratory for Condensed Matter Physics and Institute of Physics, Chinese Academy of Sciences, Beijing 100190, China<sup>7</sup>The Institute for Solid State Physics (ISSP), University of Tokyo, Chiba 277-8581, Japan

(Received 4 December 2017; revised manuscript received 9 April 2018; published 15 June 2018)

We report high-field magnetization study on the complex spin system  $h\text{-ErMnO}_3$  and propose an explanation for the  $c$ -axis phase transitions observed at 0.8, 12, and 28 T based on an analysis of the magnetization jumps, the complete  $H$ - $T$  phase diagram and the irreducible representations of the  $\text{Er}^{3+}$  ( $2a$  and  $4b$ ) spin structure. Our measurements reveal that magnetic reorientation of the representation  $\Gamma_2$  induces the magnetic transition at 12 T, i.e., from a one-third plateau phase to a fully polarized phase. The magnetic transition at 0.8 T and the anomaly at 28 T can be understood by magnetic reorientations of  $\Gamma_1 \rightarrow \Gamma_2$  and a reflection of the  $\text{Mn}^{3+}$  moments triggered by the  $\text{Er}^{3+}$  spins in strong magnetic fields. These scenarios are in good agreement with the magnetization process perpendicular to the  $c$  axis and the magnetic susceptibility results. These findings are helpful for a complete understanding of the magnetic phase transitions and the underlying physics in this family compounds.

DOI: [10.1103/PhysRevB.97.214419](https://doi.org/10.1103/PhysRevB.97.214419)**I. INTRODUCTION**

Hexagonal ( $h$ -) manganites  $\text{RMnO}_3$  ( $R = \text{Ho-Lu, Sc, Y}$ ) belong to an interesting family of type-I multiferroic materials in which magnetic and ferroelectric orders arise independently [1]. Unlike the usual type-I multiferroics, there exists a giant magnetoelectric effect in  $h\text{-RMnO}_3$  due to the strong spin-lattice couplings [2]. Recent investigations on ferroelectric domain walls discover more interesting properties, such as annular domains and topological defect for this intriguing family of compounds [3–5]. Another interest in  $h\text{-RMnO}_3$  is their unique magnetic properties. All  $h\text{-RMnO}_3$  are structurally equivalent and their magnetic properties are dominated by the  $\text{Mn}^{3+}$  and the rare-earth  $R^{3+}$  moments. The  $\text{Mn}^{3+}$  ions form layers of triangular structure stacked along the  $c$  axis, whereas the  $R^{3+}$  ions are situated at two different sites  $2a$  and  $4b$  between the layers. Figure 1 shows the crystal structure of  $h\text{-RMnO}_3$  and four possible magnetic structures of the  $R^{3+}$  spins. Owing to the strong interactions between  $\text{Mn}^{3+}$  spins and  $R^{3+}$  moments, the  $\text{Mn}^{3+}$ - $R^{3+}$  exchange, the spin-lattice coupling, and the inherent triangular frustration, this complex spin system exhibits various phase transitions and rich phase diagrams with varying temperature and magnetic fields [1,6–17].

Although extensive experiments have been performed, yet the magnetisms of  $h\text{-RMnO}_3$  are not well understood and the phase diagrams are still a matter of discussion. The

determination of the magnetic structures in these materials has been difficult because of the large unit cell, and alternative techniques have only partially clarified the symmetry of the magnetic structures. Fiebig *et al.* studied the variety of magnetic symmetries of the  $\text{Mn}^{3+}$  ions and the phase diagrams of  $h\text{-RMnO}_3$  by optical second harmonic generation (SHG) method [8–10]. In contrast, Yen *et al.* measured magnetization and dielectric constants of  $h\text{-RMnO}_3$  ( $R = \text{Ho-Yb}$ ) and found their phase boundaries extend to much higher magnetic fields [11]. For example, in  $h\text{-ErMnO}_3$  the nose shape of the phase boundary to the high-field phase was found below 4 T determined by Fiebig *et al.* [10], while this boundary was above 12 T determined by Yen *et al.* In addition, the hysteretic and the irreversible effects in SHG experiment were not observed as in the bulk magnetic and dielectric measurements. In a subsequent experiment to millikelvin, new phase boundaries were observed and the mutual induction of  $3d$  and  $4f$  orders were unveiled [12]. A recent susceptibility measurement of  $h\text{-ErMnO}_3$  under very small magnetic fields ( $\sim 30$  Oe) [13], however, suggested an antiferromagnetic ground state different from that proposed by Meier *et al.* [12]. Similar controversies were found for the phase diagrams of  $h\text{-RMnO}_3$  ( $R = \text{Ho, Tm, Yb}$ ) [9,11,14–16]. These experimental findings indicate that the magnetic properties of  $h\text{-RMnO}_3$  are much more complex than previously assumed.

So far, most studies focused on  $h\text{-HoMnO}_3$  because it shows an extremely complicated phase diagram and novel physical phenomena [14–16,18]. It is surprising that the analogous  $h\text{-RMnO}_3$  ( $R = \text{Er-Yb}$ ) have received relatively less attentions. This offers opportunity to employ experimental

\*jfwang@hust.edu.cn

†xfsun@ustc.edu.cn

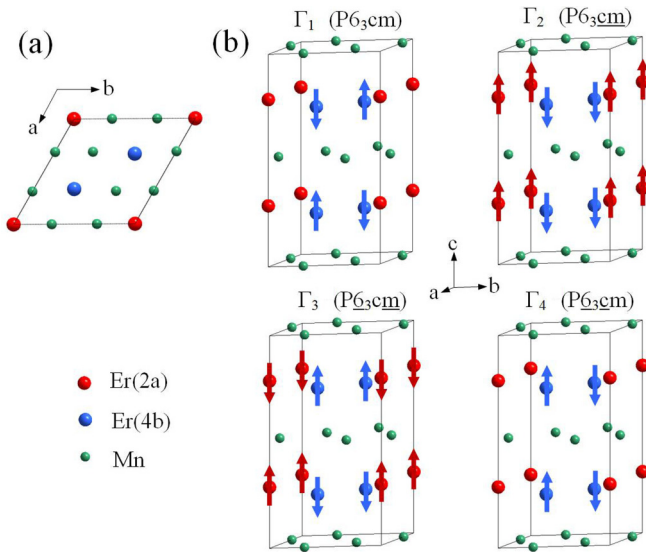


FIG. 1. Crystallographic geometry and magnetic structures of  $h$ -ErMnO<sub>3</sub>. (a) The projection along the  $c$  axis showing the actual arrangements of Er and Mn ions in the  $ab$  plane. (b) Four possible magnetic structures ( $\Gamma_1$  to  $\Gamma_4$ ) of the Er<sup>3+</sup>  $2a$  and  $4b$  lattices. The corresponding symmetry (space group) is also enclosed. Symmetry analysis shows that all emerging magnetic orders of the R<sup>3+</sup> moments can be expressed by six irreducible representations  $\Gamma_1$  to  $\Gamma_6$ . Among them,  $\Gamma_1$  to  $\Gamma_4$  are one dimensional, corresponding to the R<sup>3+</sup> moments aligned along the  $c$  axis, while  $\Gamma_5$  and  $\Gamma_6$  are two dimensional and the R<sup>3+</sup> moments lie in the  $ab$  plane. Therefore,  $\Gamma_5$  and  $\Gamma_6$  should be excluded because they cannot explain the  $c$ -axis phase transitions. We also do not show the Mn<sup>3+</sup> spin structures because they strictly orient in the  $ab$  plane and less susceptible to the field along the  $c$  axis. The details of the Mn<sup>3+</sup> and Er<sup>3+</sup> ( $\Gamma_5$ ,  $\Gamma_6$ ) representations can be referred in Ref. [12].

techniques such as high magnetic fields ( $H$ ) to explore new magnetic phase transitions in  $h$ -RMnO<sub>3</sub>. Indeed, our recent high-field magnetization measurements on  $h$ -RMnO<sub>3</sub> ( $R = \text{Er, Ho}$ ) revealed additional magnetic transitions for  $H \parallel c$  [13]. Here we report on systematical temperature dependence of the magnetization of  $h$ -RMnO<sub>3</sub> ( $R = \text{Er, Yb}$ ) single crystals in pulsed fields up to 58 T and the modified  $H$ - $T$  phase diagram for  $h$ -ErMnO<sub>3</sub>. New phase boundaries and magnetic phases are investigated in high magnetic fields. In particular, we find an effective way to analyze the magnetization data and to explain the magnetic-field-induced phase transitions observed at 0.8, 12, and 28 T according to the irreducible representations of the Er<sup>3+</sup> spin structures. The present study provides a more accurate understanding than those proposed before for this interesting material.

## II. EXPERIMENT

Single crystals of  $h$ -ErMnO<sub>3</sub> were grown by the optical floating-zone furnace with 1–2% Er element excess [19]. The crystals were characterized by the x-ray single-crystal diffraction, specific heat, and magnetic susceptibility measurements, and found to have good quality. High-field magnetization ( $M$ ) measurement was performed in Wuhan National High Magnetic Field Center using a 60 T magnet with a short pulse

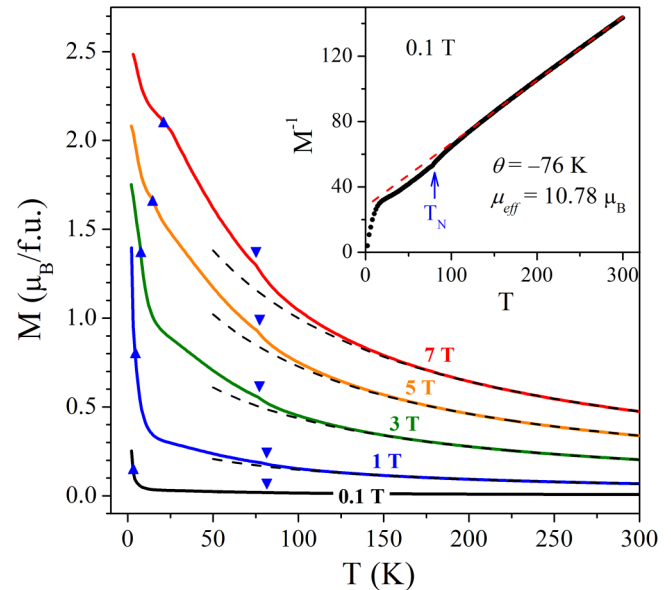


FIG. 2. Temperature dependence of the magnetization  $M(T)$  with applied magnetic field along the  $c$  axis. The symbols denote magnetic anomalies with increasing fields. The dashed (black) lines show the Curie-Weiss fitting in the temperature range of 150–300 K. Inset:  $1/M$  versus  $T$  for  $H = 0.1$  T.

of 10 ms. In the experiment, magnetization was measured by an induction method using a well-compensated pickup coil. Two pulse shots with sample-in and sample-out were carried out to subtract the spurious  $dB/dt$  signals induced by the pulsed fields.  $dM/dt$  signals from the sample were then collected and integrated as a function of magnetic fields. The high-field magnetization data were calibrated by a comparison with the low-field data measured by a commercial superconducting quantum interference device (SQUID, Quantum Design).

## III. RESULTS

Figure 2 shows the temperature dependence of the magnetization under various magnetic fields along the  $c$  axis. It is found that all curves follow a good Curie-Weiss law above 150 K. Using the relation  $\chi = C/(T-\theta)$ , where  $\theta$  is the Curie-Weiss temperature and  $C$  denotes the Curie constant, we obtained the effective moment  $\mu_{\text{eff}} = 10.78 \mu_B$ , which is in agreement with the expected value  $10.7 \mu_B$  [20]. The Curie-Weiss temperature is  $\theta = -76$  K, showing the existence of antiferromagnetic interactions at the low temperature. At about 80 K, a small anomaly is observable with a change of the slope for all the curves. This transition temperature is consistent with the Neel temperature ( $T_N$ ) of 81 K, indicating the onset of magnetic orderings of the Mn<sup>3+</sup> spins with a 120° arrangement in the  $ab$  plane [1,9]. At very low temperature at  $T_{\text{Er}} = 2.5$  K, the magnetization increases rapidly, showing the magnetic orderings of the Er<sup>3+</sup> spins along the  $c$  axis. These results are in agreement with early studies and show that the magnetic properties of  $h$ -ErMnO<sub>3</sub> are dominated by the Mn<sup>3+</sup> and Er<sup>3+</sup> ions at high and low temperatures, respectively [1,10,12].

Figure 3 shows the magnetization processes of  $h$ -ErMnO<sub>3</sub> in magnetic fields up to 30 T. For  $H \perp c$ ,  $M$  increases quickly firstly and then becomes slowly above 5 T. The  $M$  value is

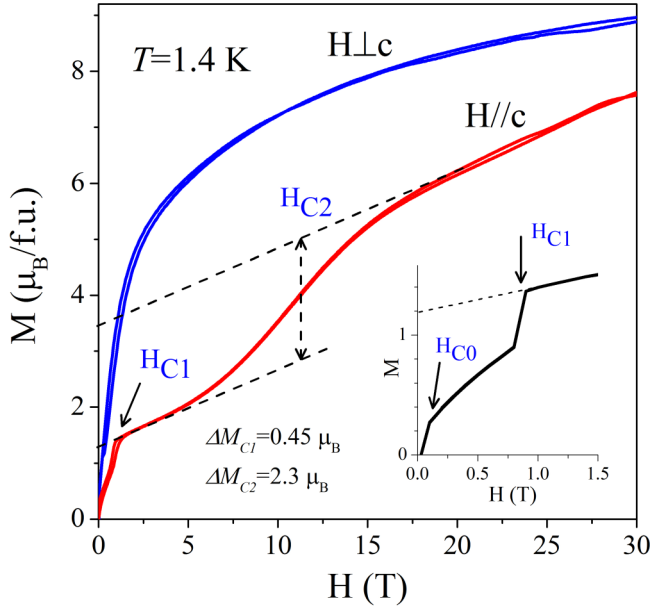


FIG. 3. High-field magnetization processes measured at 1.4 K for  $H \parallel c$  and  $H \perp c$ , where f.u. denotes the formula unit. Inset: magnetization data at 2 K for  $H \parallel c$  measured by SQUID. The arrows indicate the magnetic transitions. The dashed lines show linearly extrapolating the magnetization data to zero fields. The magnetization jump at  $H_{C1}$  ( $\Delta M_{C1} = 0.45 \mu_B$ ) is much smaller than that at  $H_{C2}$  ( $\Delta M_{C2} = 2.3 \mu_B$ ). The transition at  $H_{C2}$  is a magnetic reorientation from a one-third plateau phase to a fully polarized phase, whereas  $H_{C1}$  corresponds to a magnetic transition of  $\Gamma_1 \rightarrow \Gamma_2$  as we proposed in this paper. The magnetization jump at  $H_{C0}$  is not a real phase transition but a change from multidomains to a single domain in applied fields [12].

about  $8.9 \mu_B$  per formula unit at 30 T without going into saturation. The characteristic feature is given by the successive magnetic transitions for  $H \parallel c$ . Three transitions are observed at  $H_{C0} = 0.1$  T,  $H_{C1} = 0.8$  T, and  $H_{C2} = 12$  T, respectively. A small hysteresis is observed at  $H_{C0}$  and  $H_{C1}$  while no hysteresis is found at  $H_{C2}$ . The inset clearly shows the two sharp transitions at low fields measured at 2 K. In higher magnetic fields up to 52 T, the magnetization for  $H \parallel c$  shows another anomaly in  $dM/dH$  at  $H_{C3} = 28$  T followed by a change of the magnetization slope as shown in Fig. 4(a). This magnetic transition is evident in different pulse shots and shows a small jump in the  $M(H)$  curve. The temperature dependence of the three magnetic transitions ( $H_{C1}$ - $H_{C3}$ ) is shown in Fig. 4(b). We measured the high-field magnetization from 1.4–20 K and summarize the  $H$ - $T$  phase diagram in Fig. 5. We find that the low-field phase boundaries obtained by  $H_{C0}$  and  $H_{C1}$  together with our susceptibility data are well consistent with the results by Yen *et al.* and Meier *et al.* [11,12]. Furthermore, new phase boundaries and two additional phases separated by  $H_{C2}$  and  $H_{C3}$  are found in the high-field region. As a result, a complex phase diagram including phase I-V is constructed.

#### IV. DISCUSSION

The variety of magnetic structures in  $h$ -RMnO<sub>3</sub> can be described by either magnetic symmetries or eigenvectors of

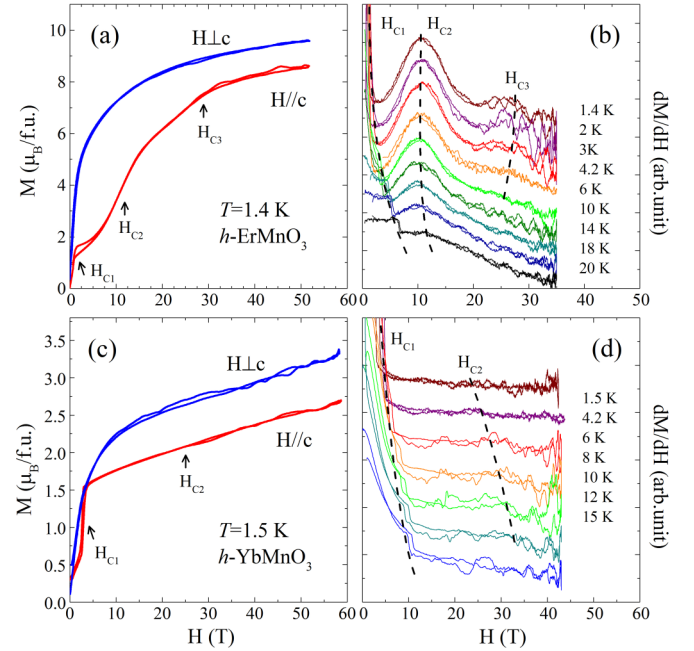


FIG. 4. (a) The magnetization measured up to 52 T and (b) The derivative  $dM/dH$  as a function of  $H$  in temperature range of 1.4–20 K for  $h$ -ErMnO<sub>3</sub>. A small magnetization jump is observed at  $H_{C3}$ , which is clearly shown in the  $dM/dH$  curves. (c) The magnetization processes for  $h$ -YbMnO<sub>3</sub> in pulsed fields up to 58 T. (d) The  $dM/dH$  curves from 1.5–15 K for  $h$ -YbMnO<sub>3</sub>. The dashed lines indicate the evolution of the magnetic transitions with temperatures.

the irreducible representations [12]. Figure 1(b) shows the four representations  $\Gamma_1$  to  $\Gamma_4$ , associated with the magnetic-field-induced ordered phases in  $h$ -ErMnO<sub>3</sub>. Briefly, we use the

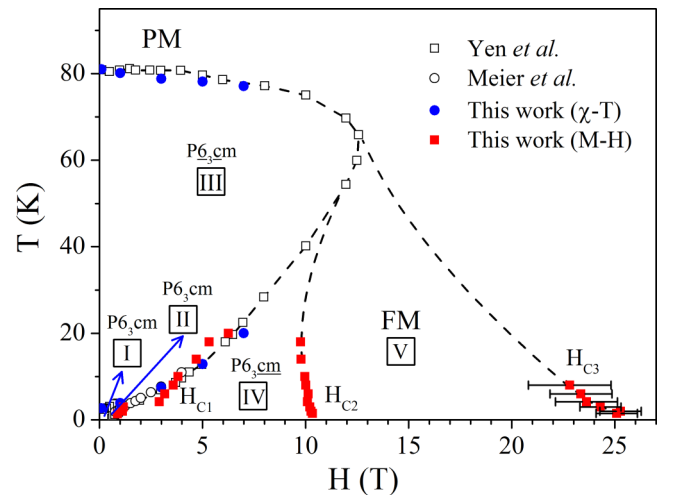


FIG. 5. The resulting high-field phase diagram of  $h$ -ErMnO<sub>3</sub>. The experimental results by Yen *et al.* and Meier *et al.* (Refs. [11] and [12]) are shown for a comparison. Five magnetic ordered phases I-V are distinguished by the phase boundaries. The dashed lines are guides for eyes. The phase V has a ferromagnetic (FM)  $\text{Er}^{3+}$  order. The boundary near 25 T is attributed to a magnetic reorientation in the  $ab$  plane where  $\text{Mn}^{3+}$  spins are triggered by the mutual induction of the  $\text{Er}^{3+}$  spins. Symmetry analysis is shown in the Appendix.

terminology of representation in the follows. The symmetry analysis will be shown in the Appendix.

Meier *et al.* studied the magnetization of  $h$ -ErMnO<sub>3</sub> in magnetic field less than 1 T and assigned the phase above  $H_{C1}$  (the phase IV) to be the Er<sup>3+</sup> ferromagnetic phase [12]. However, our high-field magnetization data show that the magnetic moment at 1 T is only about  $2 \mu_B/f.u.$ , which is much smaller than the theoretical value  $9.6 \mu_B$  of the Er<sup>3+</sup> moments. Moreover, it is hard to explain the magnetic transitions at  $H_{C2}$  and  $H_{C3}$  as explored in this paper. In our early study [13], we discussed the possibility of a spin-flop transition at  $H_{C2}$  that could activate one of two additional irreducible representations ( $\Gamma_5$  and  $\Gamma_6$ ). In this case, we find that the magnetization jump at  $H_{C1}$  will be 33% of the total Er<sup>3+</sup> moments ( $\sim 3.5 \mu_B$ ) and that at  $H_{C2}$  is relatively small, which is inconsistent with our experimental results in this work.

The accurate magnetization measurement up to 30 T is helpful for analyzing the magnetization jump and the magnetic phase transition along the  $c$  axis. In Fig. 3, the broad steplike transition at  $H_{C2}$  shows a large magnetization jump ( $\Delta M_{C2} = 2.3 \mu_B$ ) compared with that at  $H_{C1}$  ( $\Delta M_{C1} = 0.45 \mu_B$ ). Besides, the magnetization slopes on two sides of this transition are nearly the same, indicating that it is not a spin-flop but a spin-flip-like transition. By linearly extrapolating the data to zero fields, we find that the  $M$  (0 T) value almost triples across the  $H_{C2}$  transition. This scenario is reminiscent of the quantized fractional magnetization plateaus observed in frustrated magnets CuFeO<sub>2</sub> and CdCr<sub>2</sub>O<sub>4</sub> [21,22]. Usually the magnetization plateau is stabilized through the spin-lattice couplings, where a first-order phase transition occurs. Indeed,  $M(H)$  hysteresis is observed around  $H_{C1}$ , which becomes larger in a 50 T pulsed field. Upon a further inspection of  $\Gamma_1$  to  $\Gamma_4$  (Fig. 1), we find that  $\Gamma_2$  is ferrimagnetic while others are antiferromagnetic ( $M = 0$ ). Considering the unit cell as shown in Fig. 1(b), the eight Er<sup>3+</sup>(2a) spins shares four times with the nearest-neighbor unit cells. Thus the multiplicity of the 2a site is two for the Wyckoff position, while that of the 4b site remains four for one unit cell. For  $\Gamma_2$ , all the Er<sup>3+</sup>(2a) spins are antiparallel to the Er<sup>3+</sup>(4b) spins. Interestingly, we find that the net magnetic moments of  $\Gamma_2$  is  $2 \mu_{Er}$  ( $4 Er^{3+}4b - 2 Er^{3+}2a$ ) per unit cell, which is exactly 1/3 of the saturation magnetic moment  $6 \mu_{Er}$  ( $4 Er^{3+}4b + 2 Er^{3+}2a$ ). Therefore, a magnetic transition from  $\Gamma_2$  to a full alignment can realize the magnetization jump at  $H_{C2}$ , i.e., the phase IV ( $H_{C1} < H < H_{C2}$ ) is the  $\Gamma_2$  phase.

The above finding is crucial for understanding the magnetic transitions as a function of magnetic field in Fig. 4 and the resulting phase diagram in Fig. 5. It is noted that the magnetization jump at  $H_{C3}$  is negligible as seen in Fig. 4(a). Because the transition at  $H_{C2}$  to the phase V gives rise to the ferromagnetic Er<sup>3+</sup> order, the weak anomaly at  $H_{C3}$  is likely a reflection of the magnetic transition in the  $ab$  plane, where Mn<sup>3+</sup> spins are triggered by the mutual induction of the magnetic  $3d$  and  $4f$  orders in very strong magnetic fields [12]. Similar anomaly is observed in  $h$ -HoMnO<sub>3</sub> at  $\sim 40$  T and should have the same origin [13].

The magnetic ground state of  $h$ -ErMnO<sub>3</sub> has not been well identified so far. The onset of the antiferromagnetic state below 2 K is inconsistent with the representation  $\Gamma_2$  proposed by Meier *et al.* [12,13]. We notice that the magnetic moment for

$H \perp c$  is larger than that for  $H \parallel c$ . In Fig. 4(a), the  $M$  value at 52 T is about  $10 \mu_B$  for  $H \perp c$ . Given the saturation moment ( $4.9 \mu_B$ ) of the Mn<sup>3+</sup> spins, the large magnetic moment implies that the Er<sup>3+</sup> moments contribute to the magnetization process for  $H \perp c$ . For  $\Gamma_3$ , all the Er<sup>3+</sup> spins are ordered along the  $c$  axis. If it is the ground state [23], a field-induced phase transition will be observed for  $H \perp c$  due to a strong uniaxial anisotropy of the Er<sup>3+</sup> ions. However, our magnetization data do not show a magnetic transition for  $H \perp c$ . While in case of  $\Gamma_1$ , the Er<sup>3+</sup>(2a) spins are disordered. In a perpendicular field, they will give rise to a rapid increase in magnetization jump, which is in agreement with our experimental data for  $H \perp c$ , as seen in Fig. 3. The slow increase of  $M$  above 5 T should mainly come from the magnetic Mn<sup>3+</sup> moments due to a strong triangular frustration in the  $ab$  plane.

## V. CONCLUSION

We measured the magnetization of hexagonal manganite  $h$ -ErMnO<sub>3</sub> under pulsed fields up to 52 T and in the temperature range of 1.4–20 K. Consequently, a rich  $H$ - $T$  phase diagram is constructed and extends to magnetic fields higher than previously reported. By linearly extrapolating the magnetization data to zero fields, we find that the steplike transition at 12 T corresponds to field alignment from a 1/3-plateau phase to a fully polarized phase of the Er<sup>3+</sup> spins, which is essential to understand the underlying magnetism and phase transitions in  $h$ -ErMnO<sub>3</sub>. It should be noted that the magnetic ground state of  $h$ -ErMnO<sub>3</sub> is still speculative based on our careful analysis of the magnetization data. Further investigations by other experimental techniques are necessary to clarify this point.

## ACKNOWLEDGMENTS

This work was supported by National Natural Science Foundation of China (Grants No. 11574098 and No. 11474110) and the Fundamental Research Funds for the Central Universities (Grant No. 2018KFYXKJC010). X.F.S. acknowledges support from the National Natural Science Foundation of China (Grant No. U1532147), the National Basic Research Program of China (Grants No. 2015CB921201 and No. 2016YFA0300103) and the Innovative Program of Development Foundation of Hefei Center for Physical Science and Technology.

## APPENDIX

### 1. Symmetry analysis of $h$ -ErMnO<sub>3</sub>

As temperature is decreased,  $h$ -ErMnO<sub>3</sub> undergoes a phase transition at 2.5 K. The magnetic symmetry of the Er<sup>3+</sup> ions changes from P6<sub>3</sub>cm ( $\Gamma_4$ ) into P6<sub>3</sub>cm ( $\Gamma_1$ ). The reorientation of the Er<sup>3+</sup> (4b) spins induces a quick increase and then a decrease of the magnetic moments. In a  $c$ -axis field, the disordered Er<sup>3+</sup>(2a) moments lead to a rapid increase of the magnetization below 0.8 T. Because the  $H_{C0}$  transition is not a real phase transition but a magnetization process from a multidomain state [12], the symmetry of the phase II is P6<sub>3</sub>cm ( $\Gamma_1$ ). The exchange interactions between 2a and 4b spins induce a subsequent phase transition at  $H_{C1}$ , accompanied by a strong spin-lattice coupling as existing in hexagonal manganites [24,25]. The

corresponding magnetic symmetry changes from  $P6_3cm$  ( $\Gamma_1$ ) into  $P6_3cm$  ( $\Gamma_2$ ).

## 2. Magnetization study on $h$ -YbMnO<sub>3</sub>

Figures 4(c) and 4(d) present the magnetization data of  $h$ -YbMnO<sub>3</sub> single crystals in pulsed fields up to 58 T. For

$H\parallel c$ , three magnetic transitions are visible at  $H_{C0} = 0.03$  T,  $H_{C1} = 2.8$  T, and  $H_{C2} = \sim 25$  T, respectively. We find that the  $M$  value across  $H_{C1}$  ( $\sim 1.5 \mu_B$ ) is nearly 1/3 of the expected moment of the Yb<sup>3+</sup> ions ( $4.5 \mu_B$ ). This means the phase at  $H_{C1} < H < H_{C2}$  can be described by the representation  $\Gamma_2$  ( $P6_3cm$ ). We point out that  $h$ -YbMnO<sub>3</sub> has very similar phase diagram and magnetic properties with  $h$ -ErMnO<sub>3</sub>.

- 
- [1] B. Lorenz, *ISRN Condens. Matter Phys.* **2013**, 497073 (2013).
- [2] N. Hur, I. K. Jeong, M. F. Hundley, S. B. Kim, and S.-W. Cheong, *Phys. Rev. B* **79**, 134120 (2009).
- [3] J. Li, H. X. Yang, H. F. Tian, S.-W. Cheong, C. Ma, S. Zhang, Y. G. Zhao, and J. Q. Li, *Phys. Rev. B* **87**, 094106 (2013).
- [4] M. Lilienblum, Th. Lottermoser, S. Manz, S. M. Selbach, A. Cano, and M. Fiebig, *Nature Phys.* **11**, 1070 (2015).
- [5] F.-T. Huang, X. Wang, S. M. Griffin, Y. Kumagai, O. Gindele, M.-W. Chu, Y. Horibe, N. A. Spaldin, and S.-W. Cheong, *Phys. Rev. Lett.* **113**, 267602 (2014).
- [6] H. Sim, J. Oh, J. Jeong, M. D. Le, and J.-G. Park, *Acta. Cryst. B* **72**, 3 (2016).
- [7] H. Sugie, N. Iwata, and K. Kohn, *J. Phys. Soc. Jpn.* **71**, 1558 (2002).
- [8] M. Fiebig, D. Fröhlich, K. Kohn, St. Leute, Th. Lottermoser, V. V. Pavlov, and R. V. Pisarev, *Phys. Rev. Lett.* **84**, 5620 (2000).
- [9] M. Fiebig, Th. Lottermoser, and R. V. Pisarev, *J. Appl. Phys.* **93**, 8194 (2003).
- [10] M. Fiebig, C. Degenhardt, and R. V. Pisarev, *Phys. Rev. Lett.* **88**, 027203 (2002).
- [11] F. Yen, C. dela Cruz, B. Lorenz, E. Galstyan, Y. Y. Sun, M. Gospodinov, and C. W. Chu, *J. Mater. Res.* **22**, 2163 (2007).
- [12] D. Meier, H. Ryll, K. Kiefer, B. Klemke, J.-U. Hoffmann, R. Ramesh, and M. Fiebig, *Phys. Rev. B* **86**, 184415 (2012).
- [13] J. D. Song, C. Fan, Z. Y. Zhao, F. B. Zhang, J. Y. Zhao, X. G. Liu, X. Zhao, Y. J. Liu, J. F. Wang, and X. F. Sun, *Phys. Rev. B* **96**, 174425 (2017).
- [14] F. Yen, C. R. dela Cruz, B. Lorenz, Y. Y. Sun, Y. Q. Wang, M. M. Gospodinov, and C. W. Chu, *Phys. Rev. B* **71**, 180407(R) (2005).
- [15] O. P. Vajk, M. Kenzelmann, J. W. Lynn, S. B. Kim, and S.-W. Cheong, *J. Appl. Phys.* **99**, 08E301 (2006).
- [16] J. C. Lemyre, M. Poirier, L. Pinsard-Gaudart, and A. Revcolevschi, *Phys. Rev. B* **79**, 094423 (2009).
- [17] A. Midya, S. N. Das, P. Mandal, S. Pandya, and V. Ganesan, *Phys. Rev. B* **84**, 235127 (2011).
- [18] Y. J. Choi, N. Lee, P. A. Sharma, S. B. Kim, O. P. Vajk, J. W. Lynn, Y. S. Oh, and S.-W. Cheong, *Phys. Rev. Lett.* **110**, 157202 (2013).
- [19] C. Fan, Z. Y. Zhao, J. D. Song, J. C. Wu, F. B. Zhang, and X. F. Sun, *J. Cryst. Growth* **388**, 54 (2014).
- [20] M. C. Sekhar, S. Lee, G. Choi, C. Lee, and J.-G. Park, *Phys. Rev. B* **72**, 014402 (2005).
- [21] N. Terada, Y. Narumi, Y. Sawai, K. Katsumata, U. Staub, Y. Tanaka, A. Kikkawa, T. Fukui, K. Kindo, T. Yamamoto, R. Kanmuri, M. Hagiwara, H. Toyokawa, T. Ishikawa, and H. Kitamura, *Phys. Rev. B* **75**, 224411 (2007).
- [22] H. Ueda, H. A. Katori, H. Mitamura, T. Goto, and H. Takagi, *Phys. Rev. Lett.* **94**, 047202 (2005).
- [23] In our early study [13], we simply proposed the magnetic ground state ( $\Gamma_3$ ) and a phase transition at  $H_{C1}$ . Currently we find this model is not correct because it will cause a magnetization jump as large as  $\sim 33\%$  of the total Er<sup>3+</sup> moments at  $H_{C1}$ .
- [24] C. dela Cruz, F. Yen, B. Lorenz, Y. Q. Wang, Y. Y. Sun, M. M. Gospodinov, and C. W. Chu, *Phys. Rev. B* **71**, 060407(R) (2005).
- [25] X. Fabrèges, S. Petit, I. Mirebeau, S. Pailhès, L. Pinsard, A. Forget, M. T. Fernandez-Diaz, and F. Porcher, *Phys. Rev. Lett.* **103**, 067204 (2009).